NANO LETTERS

pubs.acs.org/NanoLett

Modification of Electronic Properties of Graphene with Self-Assembled Monolayers

B. Lee,[†] Y. Chen,[†] F. Duerr,[†] D. Mastrogiovanni,[‡] E. Garfunkel,[‡,§] E. Y. Andrei,[†] and V. Podzorov*[,†,§]

[†]Department of Physics, [‡]Department of Chemistry, and [§]Institute for Advanced Materials and Devices, Rutgers University, Piscataway, New Jersey 08854

ABSTRACT Integration of organic and inorganic electronic materials is one of the emerging approaches to achieve novel material functionalities. Here, we demonstrate a stable self-assembled monolayer of an alkylsilane grown at the surface of graphite and graphene. Detailed characterization of the system using scanning probe microscopy, X-ray photoelectron spectroscopy, and transport measurements reveals the monolayer structure and its effect on the electronic properties of graphene. The monolayer induces a strong surface doping with a high density of mobile holes ($n > 10^{13}$ cm^{-2}). The ability to tune electronic properties of graphene via stable molecular self-assembly, including selective doping of steps, edges, and other defects, may have important implications in future graphene electronics.

KEYWORDS Graphene, self-assembled monolayers, graphene edge functionalization, doping of graphene, transport in graphene

Self-assembled monolayers (SAMs) are ultrathin molecular films spontaneously formed at surfaces or interfaces due to chemical or physical interactions of molecules with a substrate, frequently without necessity of high-vacuum or high-temperature processing.[1] SAMs have received considerable attention due to their use in organic electronics as active materials or insulators.[1−4] Recently, it has been demonstrated that electronic properties of small-molecule and conjugated polymer organic semiconductors can be drastically modified by SAMs.[5,6] In this Communication, we report the effect of a self-assembled monolayer of (tridecafluoro-1,1,2,2-tetrahydrooctyl)trichlorosilane ($C_8H_4F_{13}SiCl_3$), or simply fluoroalkyltrichlorosilane (FTS),[7] on the electronic properties of *highly ordered pyrolytic graphite* (HOPG) and *graphene*. The latter system has attracted considerable attention due to the massless character of quasiparticles and the related novel mesoscopic transport properties.[8] Our studies using atomic-force microscopy (AFM), scanning electron microscopy (SEM), X-ray photoelectron spectroscopy (XPS), and Hall effect measurements reveal that a dense, uniform, and stable FTS SAM can be grown at the surface of graphene, inducing an excess of holes with a density of up to $n \sim 1.5 \times 10^{13}$ cm^{-2}. Such a level of doping is unattainable in conventional field-effect transistor (FET) devices. In addition, the SAM−graphene system is found to be very stable (even at elevated temperatures) in high-vacuum and ambient environment. Such robustness and the large electronic effect suggest that integration of SAM with graphene provides a new and reliable method of achieving ultrahigh doping levels in graphene.

The samples used in this study were rectangular pieces of multilayer HOPG and single-layer graphene FETs. The HOPG samples had length and width, $L \sim W = 2-5$ mm, and thickness $d = 3-20$ μm, comprising $1-6 \times 10^4$ individual layers (Figure 1). The electrical contacts to HOPG were prepared by applying colloidal graphite paint to the sides of the samples, thus forming electrical contacts to all the layers. Graphene FETs were prepared on SiO_2/n-Si wafers using mechanical exfoliation techniques and e-beam lithography (the details can be found elsewhere[9]). Before the SAM growth, devices were annealed in a flow of ultrahigh purity

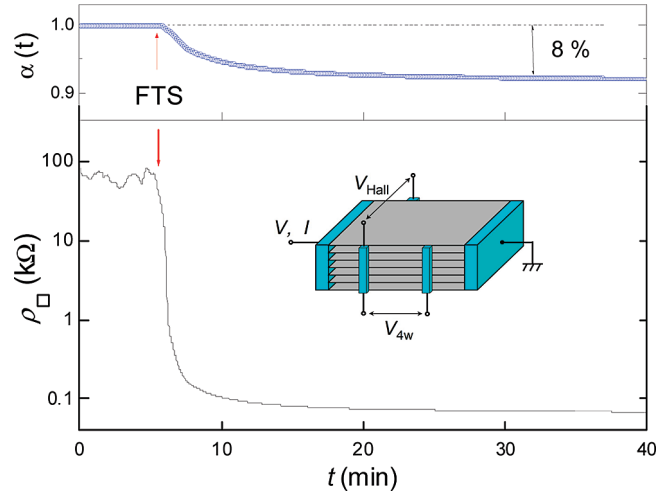

FIGURE 1. The effect of an FTS self-assembled monolayer on the resistivity of HOPG. (Top) Normalized resistivity $\alpha(t) \equiv R(t)/R_0$ of multilayer (>10^4 layers) HOPG measured as a function of FTS treatment time (initial values of R vary from sample to sample by as much as 100%). The red arrows indicate the onset of FTS exposure. (Bottom) The corresponding effect on the resistivity of an individual single layer of graphite calculated using eq 1. The sketch shows a Hall-bar sample geometry used throughout this study.

* To whom correspondence should be addressed, podzorov@physics.rutgers.edu.
Received for review: 02/18/2010
Published on Web: 00/00/0000

© XXXX American Chemical Society

DOI: 10.1021/nl100587e | *Nano Lett.* **XXXX,** *xxx,* 000–000

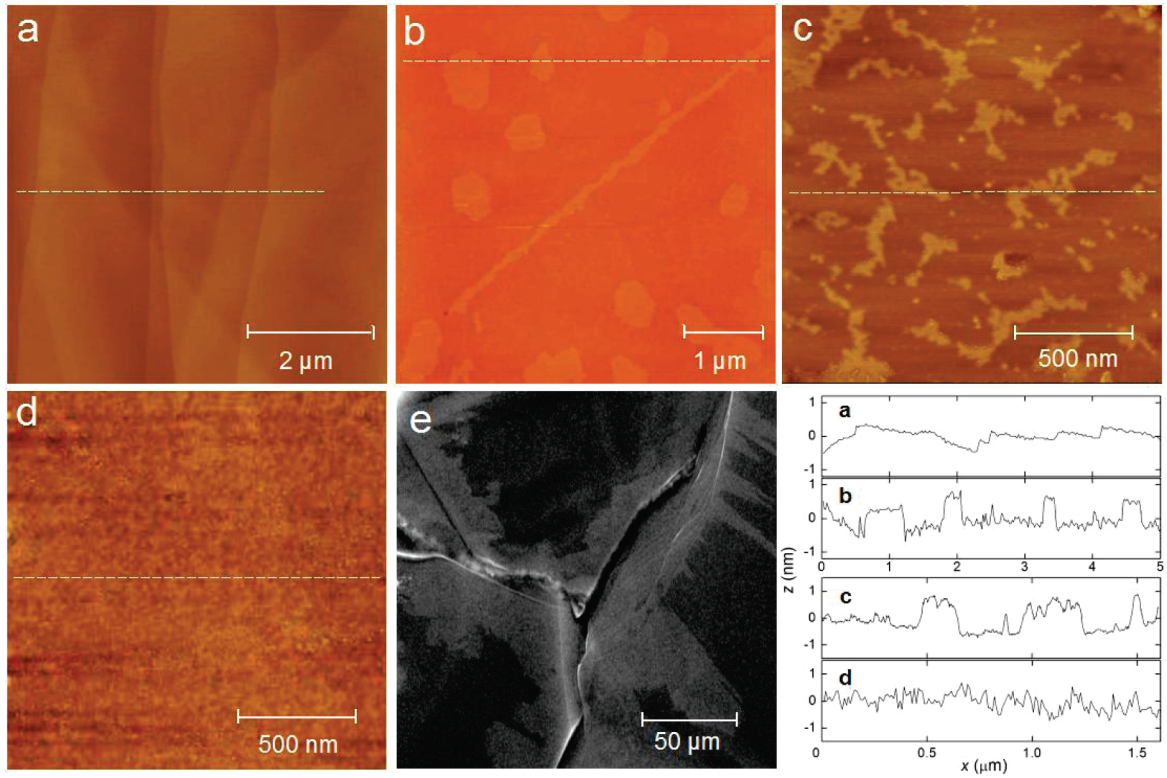

FIGURE 2. AFM (a−d) and SEM (e) images of a graphite surface functionalized with FTS SAM. (a) AFM of pristine HOPG surface (0.1 nm rms roughness); (b and c) AFM image of partially coated samples (1−2 min FTS exposure), showing different morphologies of SAM islands, including a SAM-decorated graphene edge in (b); (d) AFM of a fully coated sample (1 h exposure) showing a "fuzzy" surface morphology with 0.37 nm rms roughness; (e) a large-area SEM image of a HOPG sample partially coated with the SAM (10 min exposure), with lighter shade corresponding to SAM-coated regions. The last panel shows AFM profiles taken along the dotted lines in panels a, b, c, and d, indicating that the SAM layer is 1 nm thick.

(UHP) argon at 120 °C for 90 min and transferred under argon to the FTS growth chamber (this step is necessary for achieving a high-quality SAM on graphene). The chamber was evacuated, and then the samples were exposed to a saturated vapor of FTS. Electrical characteristics of the samples were measured in situ during the SAM growth. We have performed control experiments verifying that no intercalation of SAM molecules or any byproduct of their growth occurred in the bulk of the HOPG samples, confirming that the changes of the electrical conductivity observed are indeed due to a very strong doping of the top (exposed) graphite layer.

As the result of an FTS treatment, the resistance of HOPG samples typically decreases by 5−20%, observed both in two-probe and four-probe configurations (Figure 1, top panel). The magnitude of the decrease depends on the thickness and the initial resistance, R_0, of these macroscopically thick samples: $R(t) = \alpha(t)R_0$, where $\alpha = 0.8-0.95$ in a saturated state. Such a considerable decrease of R in samples with a typical number of layers $N = 1-6 \times 10^4$ suggests that SAM modification of the top graphite layer is very strong. Indeed, since the screening length in graphite is only ~0.5 nm,[10] only resistance of the top layer should be affected, and the sample can be represented by $N - 1$ undoped and one (top) doped layers connected in parallel. Hence, the resistivity of the top layer can be expressed as

$$\rho = \left(\frac{W}{L}\right)\frac{\alpha N}{N(1-\alpha)+\alpha}R_0 \qquad (1)$$

where the coefficient $\alpha(t) \equiv R(t)/R_0$ is determined experimentally from $R(t)$ measurements (upper panel of Figure 1). Hence, for a 3.5 μm thick sample with $N \approx 1.16 \times 10^4$ and $\alpha(t \geq 30\ \text{min}) = 0.92$ (the 8% blue curve in the upper panel of Figure 1), eq 1 gives the resistance of the top layer, $\rho_{\square}(t)$, decreasing from ~70 kΩ/□ to ~65 Ω/□ (i.e., by ~10^3 times), as the result of the SAM doping (lower panel of Figure 1).

In order to understand nanoscale morphology of the SAM−graphene system, we have performed AFM and SEM studies of partially and fully coated samples. Figure 2a shows an AFM of a pristine HOPG (~0.1 nm rms roughness): faint thin lines are ~0.3 nm high graphene steps. AFM images of a partially coated surface are shown in parts b and c of Figure 2. We have observed three types of morphology: round islands sparsely distributed on the surface (Figure 2b), ribbon-like regions corresponding to the SAM growing along the graphene steps (Figure 2b), and smaller, irregular-shaped

© XXXX American Chemical Society

DOI: 10.1021/nl100587e | *Nano Lett.* **XXXX,** *xxx,* 000–000

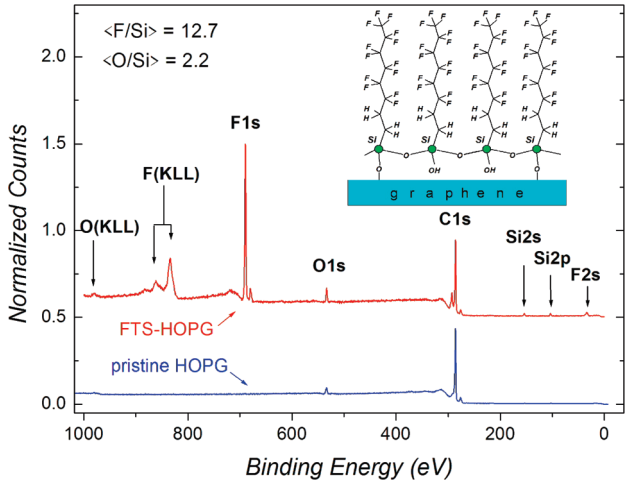

FIGURE 3. XPS of pristine (lower spectrum) and FTS-coated (upper spectrum) HOPG. Quantitative analysis based on the comparison of peak areas gives the following elemental ratios: F/Si = 12.7 ± 0.5 and O/Si = 2.2 ± 0.2 (compare with the theoretical values F/Si = 13 and O/Si = 2 for the model in the sketch). A small oxygen signal clearly present in pristine samples is consistent with oxidized graphene steps that likely play an important role in SAM nucleation. Absence of Cl in the spectra indicates that the monolayer is fully hydrolyzed. The sketch shows the suggested chemical structure of the SAM−graphene system.

islands with a higher nucleation density (Figure 2c). The topography shows that all these islands are flat regions with thickness 1.0 ± 0.2 nm, which is consistent with the length of an FTS molecule (the last panel in Figure 2). The variations in the morphology likely originate from different types and densities of defects on graphene surfaces that form SAM nucleation sites. AFM of a fully coated surface has a flat, but "fuzzy", morphology with a ~0.37 nm rms roughness (Figure 2d), which is consistent with the interaction of an AFM tip with a soft SAM. Figure 2e shows a 200 × 200 μm^2 SEM image of HOPG partially coated with FTS. A surprisingly high (for a monolayer) electronic contrast in this SEM image is likely due to the electron-rich fluoroalkyl groups of the SAM, which allows for a clear identification of the monolayer growth pattern on a large scale. In this sample, it appears that the SAM nucleation had occurred along the cracks, followed by a lateral spreading of the monolayer along the surface. These images, taken at various stages of the SAM formation, confirm that FTS forms a monolayer at graphite surface. It is worth noting that the growth is a self-limiting process, because we have not been able to observe any evidence of a second layer nucleation on top of the fully coated samples.

Elemental composition of SAM on graphite has been investigated by XPS (Figure 3). By obtaining statistics on many FTS−HOPG samples, we have concluded that a clean graphite surface is very important for successful SAM growth. We accomplished this by using a freshly exfoliated graphite samples and annealing them in a flow of UHP Ar at 120 °C for ~90 min with a subsequent transfer into the FTS chamber without exposure to air. Comparison of the areas of F 1s and Si 2p peaks of the FTS−HOPG sample (the upper spectrum) gives a F/Si ratio of 12.7 ± 0.5, which is in a good agreement with the actual molecular stoichiometric ratio of 13.

XPS also helps to understand the growth mechanism of silane SAMs on graphite. According to the trichlorosilane chemistry on SiO_2, FTS molecules first undergo hydrolysis in the presence of water at the surface or in a vapor phase, and all three chlorine atoms are replaced by hydroxyl groups (OH). One of them then covalently bonds to the OH-terminated Si substrate by forming a Si−O−Si bond. The other two OH groups covalently bond to the adjacent FTS molecules via Si−O−Si links formed in a similar fashion.[7] Here, we propose a similar, but somewhat different, growth mechanism for the FTS−graphite system.

First, our XPS data show no chlorine signal in the fully coated samples (the Cl peak would have appeared at ~200 eV in the upper spectrum), indicating that FTS undergoes a complete hydrolysis, and HCl byproduct is removed from the system. We believe that the source of water in our experiment is the residual gas in the SAM treatment chamber (the base pressure before the SAM deposition is about 3 × 10^{-3} Torr). Annealing of the samples in Ar prior the SAM growth, on the other hand, helps to remove some organic contaminants and excess of water from the surface of graphite. This last point is very important, because in a separate control experiment, no SAM could be grown on the samples intentionally incubated in a water vapor bath, indicating that too much water at the surface is detrimental for the SAM growth.

Second, a small O 1s signal is clearly observed in all freshly exfoliated HOPG samples (the lower spectrum) is consistent with only the graphene steps being oxidized. Oxygenated species, such as graphene oxide, hydroxyl, or carboxyl groups, may play a key role in SAM nucleation on graphite. Initially, FTS molecules covalently anchor to these defects, and once such nucleation sites are formed, other FTS molecules covalently attach to them via Si−O−Si bonds, without forming strong bonds to the substrate. This process, known in silane chemistry as 2D self-polymerization, does not require surface oxygen, except for oxygen species at the anchoring sites.[7] As a result, most of the FTS molecules in the monolayer are covalently bonded to the neighboring FTS molecules, but only a few are covalently bonded to the graphite substrate (sketch in Figure 3). The Si/O ratio for the fully coated samples obtained from our XPS spectra is 2.2 ± 0.2. According to the silane chemistry,[7] in an ideal monolayer, each Si atom is connected to three O, two of which are shared between the adjacent FTS molecules in a 2D polymerized network (sketch in Figure 3). In such a structure, the expected Si/O ratio is 2. For an unpolymerized, yet fully hydrolyzed, trichlorosilane, the expected Si/O ratio is 3. Therefore, our XPS data suggest that in the SAM−graphene system FTS undergoes a complete hydrolysis and forms an almost fully cross-linked interconnected 2D SAM network

© XXXX American Chemical Society

DOI: 10.1021/nl100587e | *Nano Lett.* **XXXX,** *xxx,* 000–000

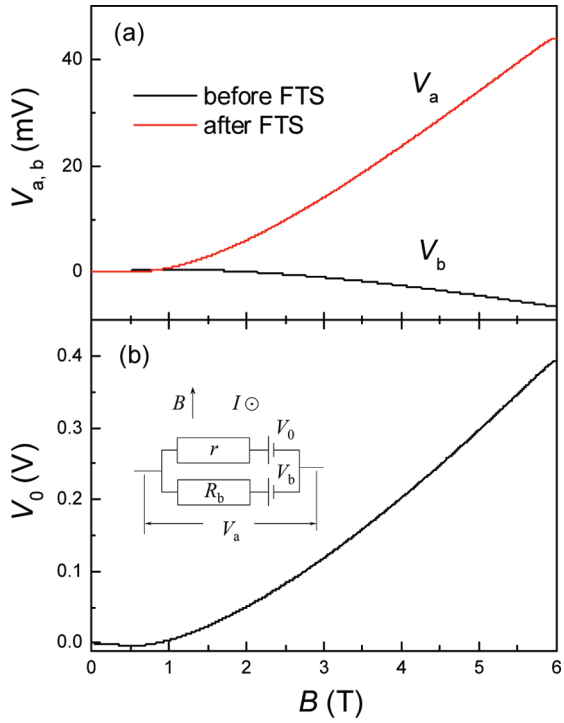

FIGURE 4. Hall effect measurements of graphite functionalized with an FTS SAM. (a) Hall voltage of a HOPG sample measured before (black) and after (red) FTS treatment. A clear change of sign at $B \sim 1$ T is observed. (b) Hall voltage of a SAM-doped single-layer graphite extracted from panel a using eq 2 and the corresponding circuit model (depicted).

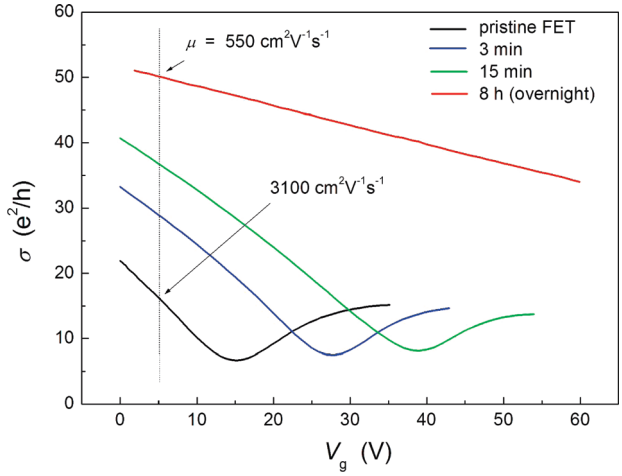

FIGURE 5. Evolution of transconductance characteristics, $\sigma(V_g)$, of a graphene FET measured in situ as an FTS SAM grows on a graphene surface. The data have been collected at different growth times: 0 (pristine graphene), 3 min, 15 min, and 8 h. Mobilities of the pristine graphene FET and the same device treated overnight are 3100 and 550 cm^2 V^{-1} s^{-1}, respectively (calculated at $V_g = 5$ V).

(Figure 3). The fact that no Cl signal is detected in XPS measurements provides solid proof that the observed doping effect is not induced by Cl byproducts of the SAM formation.

To further investigate the effect of the SAM on the electronic properties of graphite, we have carried out Hall effect measurements of HOPG before and after the FTS growth. Although the change in the resistance of HOPG samples is only a few percent because of a large number of unaffected layers (Figure 1), the situation is drastically different in the Hall measurements. Figure 4a shows the Hall voltage measured in a typical HOPG sample. The most prominent feature is a different sign of the Hall voltage at $B > 1$ T. In addition, the magnitude of the Hall voltage becomes much larger after FTS treatment. A SAM-coated HOPG sample can be represented by two parts connected in parallel: a highly conductive hole-doped top layer and a bulk. As a semimetal, pristine HOPG has a gapless multielectronic-band structure. The sign of the Hall voltage measured in HOPG samples is determined by the relative amount of electrons and holes. At high magnetic fields, the electron and hole bands become separated by a gap of several tens of millielectronvolts.[11] As a result, transport in HOPG becomes dominated by one type of carrier that defines the sign of the Hall voltage. The sample in Figure 4a shows a negative Hall voltage before FTS treatment, which in our experimental setup corresponds to predominantly electron conduction. After FTS treatment, the Hall voltage becomes positive, indicating the addition of holes to the sample. The inset in Figure 4b shows a model of the Hall effect in FTS-coated HOPG: the transverse (i.e., Hall) voltages and longitudinal resistances are shown with an excitation current perpendicular to the page. The top layer, dominated by the SAM-induced holes, has a longitudinal resistance $r(B)$ and generates a Hall emf V_0, when the magnetic field is applied. The HOPG bulk has a longitudinal resistance $R_b(B)$ and a Hall emf V_b. The total Hall voltage after FTS coating, V_a, is a function of these four parameters. By combining the measured Hall voltages and magnetoresistance values $r(B)$ and $R_b(B)$ (not shown here for simplicity) before and after FTS growth, we can extract the contribution of the top (doped) layer to the Hall effect

$$V_0 = V_a + (V_a - V_b)r(B)/R_b(B) \qquad (2)$$

The extracted V_0 is plotted in Figure 4b. As expected, V_0 has a positive sign at high magnetic fields, corresponding to hole doping. As a first approximation, we apply the equation for a conventional band-semiconductor Hall effect to the nearly linear section of $V_0(B)$ in Figure 4b, $\Delta V_0 = \Delta B I_0/(\mathbf{e}n)$, where the longitudinal current is $I_0 = (W/L)\sigma_\square V_{SD}$ and $\sigma_\square = \mathbf{e}n\mu$, and obtain the hole density $n = 1.4 \times 10^{13}$ cm^{-2} and hole mobility $\mu = 3700$ cm^2/(V s). Such remarkable carrier density is difficult to achieve electrostatically in FETs.

We have also performed FTS growth and electrical measurements on single-layer graphene FETs. Several samples were studied and showed similar results. The transconductance of graphene FETs, $\sigma(V_g)$, was monitored in situ, as FTS SAM was growing on the surface of the sample (Figure 5). These devices show only a minor hysteresis in V_g sweeps (much smaller than the effect of SAMs reported below), and

© XXXX American Chemical Society

DOI: 10.1021/nl100587e | *Nano Lett.* **XXXX,** *xxx,* 000–000

hence for clarity we show the data recorded in one (positive) direction of the V_g sweep. There are several important observations: (1) the initial Dirac point of pristine graphene is at $V_g = 15$ V but shifts to more positive V_g as the SAM is growing and eventually goes beyond the experimentally accessible range of gate voltages; (2) away from the Dirac point, the conductivity shows a sublinear increase with V_g, both for pristine and briefly treated samples ($\leq$15 min), but becomes linear for a saturated monolayer SAM coverage (longer treatments); (3) the conductivity of graphene increases with FTS growth, while the field-effect mobility decreases.

A nonzero V_g of the Dirac point in as-prepared graphene is usually understood in terms of unintentional doping by species absorbed from the ambient.[12,13] As the FTS SAM is grown on graphene, the Dirac point is shifted toward more positive V_g, indicating that holes are induced in the sample at a density $\Delta n = \gamma \Delta V_g^{\text{Dirac}}$, with $\gamma = 7.2 \times 10^{10}$ cm^{-2} V^{-1}. The most significant and rapid changes in the electrical characteristics of the devices occur within the first ~60 min of the FTS growth (correlated with the time scale of the monolayer formation), after which the process slows down and saturates. To make sure that all the possible "pin-holes" are sealed by the SAM, we have prepared fully coated samples by an overnight FTS treatment. For a complete SAM (red curve in Figure 5), the position of the Dirac point is estimated by extrapolating the experimentally accessible linear portion of the curve to a minimum conductivity of ~7 e^2/h, leading to a density of SAM-induced holes, $\Delta n \approx 1.2 \times 10^{13}$ cm^{-2}, close to the value obtained from our Hall effect measurements.

Observations (2) and (3) above can be explained by the model of long-range Coulomb scattering due to charged impurities, in which long-range scattering leads to a linear dependence of σ on carrier density, whereas short-range scattering results in a sublinear dependence.[14−16] FTS extracts electrons from graphene, which converts SAM molecules into negatively charged static centers interacting with mobile holes through a long-range Coulomb interaction. Correspondingly, in Figure 5, the $\sigma(n)$ dependence changes from sublinear to linear with μ decreasing, as more and more SAM molecules are introduced onto the surface, and the dominant scattering mechanism becomes long-range Coulomb interactions with charged impurities. The theory of long-range scattering in graphene also shows that mobility is inversely proportional to the density of scattering centers: $\mu = 1.1 \times 10^{15} \varepsilon / n_{\text{imp}}$, where ε is the dielectric constant of the material that contains scattering centers[15] (ε of an FTS monolayer is estimated to be ~3.5[17]). Combining these results, we can estimate the density of SAM-related scattering centers for a complete monolayer on graphene: $n_{\text{imp}} = 0.67 \times 10^{13}$ cm^{-2}, i.e., about 1/2 of the density of SAM-induced holes. This result is not unexpected, since the FTS SAM is a dense cross-linked layer, and FTS molecules may not necessarily be treated as independent scatterers.

After initial measurements, the FTS−graphene devices were left in ambient air (relative humidity ~60−70%) for more than 1 week and then remeasured. The FTS-induced conductivity decreased by only a few %, compared to the result obtained on freshly coated samples while still in vacuum. In addition, neither the monolayer nor the SAM-induced conductivity has been destroyed by annealing FTS−graphene devices in forming gas at 120 °C. These stability tests indicate that the SAM−graphene system is very stable even at elevated temperatures.

There is a qualitative agreement between our results on HOPG and graphene FETs: in both cases a strong p-type doping with a large carrier density has been observed. The quantitative differences in the SAM-induced single-layer σ in these cases might arise from: (a) different band structures of an isolated graphene and multilayered graphite, (b) different relative weights of various scattering mechanisms, and (c) an extra scattering in graphene FETs caused by the underlying SiO_2.

It is worth noting that our observation of SAM decoration of graphene edges (Figure 2b) confirms the hypothesis of edge termination with oxygen species.[18] Indeed, according to the trichlorosilane chemistry on SiO_2, such groups as hydroxyl (OH) or carboxyl (COOH) are necessary for the SAM molecules to covalently bond to the surface.[19] Our observation suggests that the mechanism of SAM formation on graphene is based on a defect-mediated nucleation, followed by a lateral 2D polymerization that eventually leads to a complete monolayer coverage by a cross-linked and robust 2D siloxane network (model in Figure 3). As opposed to doping by electropositive atoms such as alkali ions,[20] SAM doping of graphene exhibits an excellent stability in ambient and high-vacuum environments. The distinct morphology of SAM nucleation suggests that it can be used as a simple technique for visualization or electronic passivation of graphene edges and defects, as well as for complete SAM coverages. Although the mechanism of SAM-induced doping is not yet fully understood, we speculate that free silanol groups (Si−OH) at the SAM−graphene interface might be responsible for a strong *protonic doping* of the surface due to high acidity of the protons. Interestingly, our preliminary measurements show that exposure to polar gases (such as vapors of common solvents) reversibly change the SAM-induced conductivity of graphene, which is very promising for development of novel chemical sensors.

In conclusion, we have synthesized stable self-assembled monolayers of fluoroalkyl silanes at the surface of graphite and graphene, resulting in a strong surface doping effect of graphene with carrier densities in excess of 10^{13} cm^{-2}. Nanoscale imaging and X-ray photoelectron spectroscopy confirm a simple monolayer structure with the predicted stoichiometry. The novel doping approach described here offers the potential for chemical modification of graphene electronic properties using methods of molecular engineering and self-assembly.

© XXXX American Chemical Society

DOI: 10.1021/nl100587e | *Nano Lett.* **XXXX,** *xxx,* 000−000

Acknowledgment. We thank X. Du, D. Maslov, M. E. Gershenson, and L. C. Feldman for helpful discussions, T. Choi and S.-W. Cheong for access to AFM, and J. Paramanandam for help on SEM imaging. V.P. acknowledges support through NSF-ECCS-0822036 and NSF-DMR-0843985. E.Y.A. acknowledges support through NSF-DMR-0906711.

REFERENCES AND NOTES

(1) Di Benedetto, S. A.; Facchetti, A.; Ratner, M. A.; Marks, T. J. Molecular Self-Assembled Monolayers and Multilayers for Organic and Unconventional Inorganic Thin-Film Transistor Applications. *Adv. Mater.* **2009**, *21*, 1407–1433.

(2) Kobayashi, S.; et al. Control of carrier density by self-assembled monolayers in organic field-effect transistors. *Nat. Mater.* **2004**, *3*, 317–322.

(3) Takeya, J.; et al. Effect of polarized organosilane self-assembled monolayers on organic single-crystal field-effect transistors. *Appl. Phys. Lett.* **2004**, *85*, 5078–5080.

(4) Campbell, I. H.; Kress, J. D.; Martin, R. L.; Smith, D. L.; Barashkov, N. N.; Ferraris, J. P. Controlling charge injection in organic electronic devices using self-assembled monolayers. *Appl. Phys. Lett.* **1997**, *71*, 3528–3530.

(5) Calhoun, M. F.; Sanchez, J.; Olaya, D.; Gershenson, M. E.; Podzorov, V. Electronic functionalization of organic semiconductors with self-assembled monolayers. *Nat. Mater.* **2008**, *7*, 84.

(6) Kao, C.-Y.; Lee, B.; Wielunski, L. S.; Heeney, M.; McCulloch, I.; Garfunkel, E.; Feldman, L. C.; Podzorov, V. *Adv. Funct. Mater.* **2009**, *19*, 1906.

(7) Hydrophobicity, hydrophilicity and silane surface modification, Gelest brochure, www.gelest.com, 2006.

(8) Castro Neto, A. H.; Guinea, F.; Peres, N. M. R.; Novoselov, K. S.; Geim, A. K. The electronic properties of grapheme. *Rev. Mod. Phys.* **2009**, *81*, 109–162.

(9) Du, X.; Skachko, I.; Barker, A.; Andrei, E. Y. Approaching ballistic transport in suspended graphene. *Nat. Nanotechnol.* **2008**, *3*, 491.

(10) Visscher, P. B.; Falicov, L. M. *Phys. Rev. B* **1971**, *3*, 2541.

(11) Sercheli, M. S.; Kopelevich, Y.; da Silva, R.; Torres, J. H. S.; Rettori, C. *Solid State Commun.* **2002**, *121*, 579.

(12) Tam, Y. W.; et al. Measurement of Scattering Rate and Minimum Conductivity in Graphene. *Phys. Rev. Lett.* **2007**, *99*, 246803.

(13) Novoselov, K. S.; et al. Two-dimensional gas of massless Dirac fermions in graphene. *Nature* **2005**, *438*, 197–200.

(14) Hwang, E. H. Carrier Transport in Two-Dimensional Graphene layers. *Phys. Rev. Lett.* **2007**, *98*, 186806.

(15) Chen, J.-H.; et al. Charged-impurity Scattering in Graphene. *Nat. Phys.* **2008**, *4*, 377–381.

(16) Adam, S.; Hwang, E. H.; Galitski, V. M.; Das Sarma, S. A self-consistent theory for graphene transport. *Proc. Natl Acad. Sci. U.S.A.* **2007**, *104*, 18392.

(17) Allison, D. Lee, B. Podzorov, V., Frisbie, C. D. In preparation.

(18) Wang, X.; Tabakman, S. M.; Dai, H. *J. Am. Chem. Soc.* **2008**, *130*, 8152.

(19) Sagiv, J. Organized monolayers by adsorption: formation and structure of oleophobic mixed monolayers on solid surfaces. *J. Am. Chem. Soc.* **1980**, *102*, 92.

(20) Chen, J.-H.; et al. *Nat. Phys.* **2008**, *4*, 377.

© XXXX American Chemical Society

DOI: 10.1021/nl100587e | *Nano Lett.* **XXXX,** *xxx,* 000–000